Multi-scale modeling of aging of waspaloy superalloy: prediction of microstructure evolution and coupling with mechanical properties

Betül Gövercin*[1,2], Caner Şimşir[1,2]

Ni-based superalloys operating under challenging conditions require high mechanical strength at elevated temperatures where heat treatment processes are crucial for those materials including solutionizing and aging. The yield strength of these alloys arises concurrently from different strengthening mechanisms and the main strengthening mechanism for an alloy can change depending on the composition and processing methods. Starting from solidification, the optimum solutionizing temperature for Waspaloy is determined and isothermal aging parameters were set with ICME methods where results were compared with physical experiments. By using the modeling results, yield strength estimation was conducted from room temperature to operational temperatures and validated with thermomechanical experiments. Orowan and coherency strengthening were each found to have a great impact on yield strength, showing the importance of heat treatment processes on Waspaloy. The methods described and the model developed can be used for refining composition and microstructure to have the desired strength.

KEYWORDS: WASPALOY - NI-BASED SUPERALLOY - HEAT TREATMENT - PANDAT™ - MODELING

INTRODUCTION

Ni-based superalloys are designed and developed to operate under high temperatures, high mechanical loads, and corrosive environments, in regard to the Brayton cycle where higher efficiency systems such as turbine engines are required (1). To provide these challenging properties, these materials are designed by including many alloying elements for phase transformations that contribute to corrosion resistance and material strength at elevated temperatures arising from solid solution hardening and grain boundary strengthening of γ-matrix, precipitation hardening, and coherency strengthening due to γ' particles. Heat treatment processes adequately designed have a great impact on overall strength with respect to the amount and distribution of $L1_2$ γ' particles. Since there are many different mechanisms contributing to overall strength, establishing a physically based model becomes more crucial in alloy design fields due to the difficulty of investigating the contribution of each strengthening mechanism in experiments by isolating the mechanism

Betül Gövercin, Caner Şimşir
Middle East Technical University,
Simultura Material Technologies Inc, Türkiye
betulgovercin@simultura.com

which is also affected by chemical composition and phase fractions.

The coherency and solid solution strengthening contribution on overall yield strength is found to be a subject open for discussion in some studies (2-11); however, according to the authors' knowledge, coherent and semi- coherent particles' interaction with ɣ-matrix and strain fields occurring due to substitutional and interstitial alloying atoms create obstacles for dislocation movement and increases the material strength. Therefore, the combined effects of grain boundary, coherency, and solid solution strengthening should be considered to predict the yield strength of the material.

Although computational alloy design studies with related software give a prediction on yield strength, the results obtained in such simulations have shown overprediction where optimization of the heat treatment parameters to obtain desired properties is crucial for the design of such materials.

In this study, isothermal aging of Waspaloy is applied to model the effect of each strengthening mechanism calculated by using the thermodynamic and precipitation modeling outputs. For the validation of modeling studies, physical experiments were performed both at room temperature and around operational conditions. The model is expected to be used in alloy design in the future for the optimization of material performance with the related composition and microstructure.

METHOD

Chemical, Microstructural, and Thermomechanical Experiments

To investigate the microstructural variations during heat treatment and predict the yield strength accordingly, the composition of the as-received Waspaloy was analyzed with optical emission spectroscopy (OES) from 5 different locations on diameter.

Tab.1 - Chemical composition of the as-received Waspaloy (without P and S).

Element	Al	B	C	Cr	Co	Fe	Mo	Si	Ti	Ni
Mean wt%	1.44	0.01	0.06	18.9	13.1	0.29	4.34	0.02	2.85	Bal.

Since the ingot studied was procured in hot forged condition, the microstructure of the as-received ingot was also analyzed from the same 5 locations with optical microscopy (OM) for the determination of mean grain size in accordance with ASTM E-112 and secondary electron microscopy (SEM) together with energy dispersive spectrometry (EDS) for microstructural analysis including ɣ', carbide size and amount determination that will affect the desired time for solutionizing. The samples were cut with electrical discharge machining (EDM) and embedded in conductive bakelite. Grinding with SiC abrasive papers and polishing with diamond suspensions were applied for surface preparation. All samples were etched with 2 gr $CuSO_4$ + 40 ml HCl + 40 ml Ethanol (95%) etchant (12).

Heat treatment applications at 1080°C for 1-hour for solutionizing followed by water quenching and aging at 850°C for 18-hours followed by water quenching were conducted with THERMNEVO – Nevola Curing Furnace on 12 mm diameter rods prepared with EDM. After solutionizing and aging, high-resolution transmission electron microscopy (HRTEM) was used for the ɣ' fraction and size determination. The samples cut in 0.35 mm thickness were used for the extraction of 3mm diameter discs by using a disc punch and further prepared with grinding and twin-jet electrolytic polishing with 10 vol. % perchloric acid at 20.5V at -5°C.

Aged samples were subjected to CNC machining for tensile test preparation with SMR311 geometry. Gleeble 3800 system was used for tensile testing at room temperature, 580°C, 650°C, and 720° with 10^{-3} strain rate.

Solidification Modeling

The PANDAT™ software with the PanNi2023_all database and chemical composition given in Table 1 were used to predict the equilibrium and Scheil solidification phase compositions and phase fractions in regard to the CALPHAD method. The thermodynamic equilibrium of a given system with multiphase equilibria at constant pressure is determined with respect to the summation of molar Gibbs energies of the stable phases, leading to minimum Gibbs energy.

$$G = \sum_{\varphi} n^{\varphi} G_m^{\varphi} \quad (1)$$

In the given formula above, $n\phi$ stands for the number of moles and $G\phi_m$ is for the molar Gibbs energy of phase ϕ (13).

In the Scheil method, it is assumed that the diffusion in the liquid takes place at an infinite rate and there is no diffusion in the solid phases where equilibrium is held at the liquid-solid interface. (14-16). The solute profile can be found as:

$$C_s = kC_0(1 - f_s)^{(k-1)} \quad (2)$$

where C_S is the concentration of solute in the solid, at a fractional distance along the bar, f_S, C_0 is the initial concentration of the liquid, and k is the partition coefficient.

Precipitation Modeling

The CALPHAD method is developed to perform thermodynamic calculations and determine the phase diagrams accordingly. As this method is improved in time, applying kinetic calculations has also become possible by using the related databases formed either experimentally or together with ab-initio calculations. The PANDAT™ software with the PanNi2023_all database and chemical composition given in Table 1 were also used in this part of the modeling study and the kinetic database for Waspaloy is constructed by using the property model calculation results conducted by PANDAT™. The input data for the precipitation modeling studies are given in Table 2, below. The molar volume, interfacial energy, dislocation density and atomic spacing values are obtained from the property model calculation results of PANDAT™. Grain size is determined by using the as-received ingot as mentioned in Part 2.1; the aspect ratio and contact angle for the precipitates were used as the default values which is applicable to almost all the Ni-based superalloys. By using these parameters, aging modeling is performed at 850°C for 18-hours by using the KWN model.

Tab.2 - Input parameters for precipitation modeling of Waspaloy by using PANDAT™.

Simulation Parameter	ɣ-matrix	ɣ' precipitates
Molar Volume [m^3/mole]	7.1E-6	7.1E-6
Grain Size [μm]	35	-
Dislocation Density [m^{-2}]	1E-12	-
Aspect Ratio	1	1
Interfacial Energy [J/m^2]	-	0.030
Atomic Spacing [m]	-	3.621E-10
Contact Angle [°]	-	90

Langer-Schwarz-Kampmann-Wagner approach also known as KWN (Kampmann-Wagner Numerical model) is used which is a mean-field model assuming that the nucleation takes place homogeneously through the matrix and the precipitates form in spherical shape (17-22).

The nucleation rate [3] and growth rate [4] with the KWN model are constructed with the formula:

$$J(t) = J_s \exp\left(-\frac{\tau}{t}\right) = Z\beta^* N_0 \exp\left(-\frac{\Delta G^*}{kT}\right) \exp\left(-\frac{\tau}{t}\right) \quad (3)$$

$$\frac{dR}{dt} = \frac{C(t) - C_R}{C_P - C_R} \frac{D}{R} \quad (4)$$

Where J_s is stationary nucleation rate, τ is incubation time, N_0 is number of potential nucleation sites per unit volume, $\beta*$ is the rate of solute atoms in matrix joining the nucleus, C_p is the concentration of the solute in the precipitate, $C(t)$ is the concentration of the solute in the matrix and C_R is the concentration of the solute in the interface boundary.

Yield Strength Modeling

The overall yield strength is obtained by summing Orowan strengthening due to dislocation looping around the precipitates (σ_{oro}), coherency strengthening arising from lattice misfit between matrix and precipitates (σ_{coh}), solid solution strengthening of γ matrix (σ_{ss}), grain size/ boundary strengthening (σ_{gh}) and lattice strength of pure nickel (σ_0).

$$\sigma_y = \left(\sigma_{ss}^n + \sigma_{ph}^n + \sigma_{Oro}^n + \sigma_{gh}^n + \sigma_{coh}^n + \sigma_0^n\right)^{1/n} \quad (5)$$

The linear summation method is applied by taking n=1 has been found to show a better fit with experimental data.

Precipitation Hardening

Precipitation hardening mechanisms such as particle cutting and bowing were explained with the implementation of the role of dislocations (23-25). In the case where the applied stress is smaller for the penetration of dislocations to precipitates - usually, the incoherent precipitates with larger precipitate sizes are seen in the microstructure -, Orowan bowing is seen in the microstructure where the dislocations with lower stress bow between the particles (26,27). An extended equation for the calculation of Orowan dislocation looping strengthening is also introduced as (28-30):

$$\Delta\sigma_{orowan} = M\frac{0.4Gb}{\pi\sqrt{1-\upsilon}}\frac{ln\left(2\sqrt{\frac{2}{3}}r/b\right)}{\lambda} \quad (6)$$

$$\lambda = 2\sqrt{\frac{2}{3}}r\left(\sqrt{\frac{\pi}{4f}} - 1\right) \quad (7)$$

where G is matrix shear modulus, υ is the Poisson's ratio of the matrix, f is the volume fraction of precipitates, r is the mean radius of precipitates, λ is mean interparticle spacing and b is burgers vector.

Coherency Strengthening

Due to the cutting of particles or with the looping of dislocations around the precipitates, Ni-based superalloys are mostly hardened with the precipitation of γ' phase. Although those mechanisms rely on the antiphase boundary hardening occurring from the coherency of γ', some studies are conducted to investigate the effect of the coherency strains arising from the lattice misfit on the overall yield strength of the material. Strengthening due to lattice misfit arises from the stress fields around the interface at which the precipitate is coherent with the matrix. Those stress fields restrict the dislocation gliding, and the contribution of this misfit is explained by Brown and also by (23,24,30):

$$\sigma_{misfit} = MxG(\varepsilon)^{3/2}\sqrt{2f\frac{r}{b}} \quad (8)$$

$$\varepsilon = |\delta|\left[1 + 2G\left(1 - 2v_p\right) / G_P(1 + v_P)\right] \quad (9)$$

$$\delta = \frac{a_P - a}{a}$$

$$\delta = \frac{a_P - a}{a} \quad (10)$$

where χ is material constant changing from 2 to 3, ε is the misfit strain parameter, G_p is shear modulus of precipitates and υ_p is the Poisson's ratio of the precipitates, δ is the difference between lattice parameters of precipitate a_p and matrix a.

Solid solution strengthening

Strengthening due to solid solution occurs when the solute element with higher strength dissolves in the solvent metal and either replaces the host atom or places between the host atoms, causing localized lattice distortions. These distortions interact with the dislocations and strengthen the material either by dislocation locking due to size mismatch, modulus mismatch, and stacking-fault interaction, or dislocation friction (31-35)

The solid solution strengthening formula varies for the ordered and disordered phases (36-38). Since both ɣ-matrix and ɣ' precipitates have ordered structures, below formula introduced by Fleischer can be used for the prediction of strength contribution via solid solution (39):

$$S_i^{\gamma} = \left(f_{\gamma}\right)\left[\Sigma\beta_i^{\gamma}(x_i^{\gamma})\right]^{\frac{1}{2}} \quad (11)$$

Where β_i^{γ} is a constant set for each element and depends on the atomic size and modulus, x_i^{γ} is the atomic percent of the element in the ɣ-matrix.

Grain boundary strengthening

Grain boundary strengthening is often explained by blocking the dislocation motion by absorbing its energy or dividing the dislocations into pieces due to the misorientation between consecutive grains in polycrystalline materials. The grain size effect on yield strength is described by the Hall-Petch equation (40):

$$\sigma_{gh} = \frac{k_y}{\sqrt{D}} \quad (12)$$

Where k_y is the Hall-Petch constant that varies depending on the alloy and D is the grain size.

RESULTS AND DISCUSSION

In order to define the solutionizing and aging temperature for Waspaloy, solidification under equilibrium and non-equilibrium conditions is analyzed. As the as-received specimen's chemical composition is compared with the patent, it is observed that the amounts of all the alloying elements were within the limits.

With the obtained chemical composition from OES, equilibrium cooling solidification is conducted between 500 to 1750°C as given in Table 3-a and it is observed that the Waspaloy for the given composition is expected to fully solidify with a low amount of TiC and ɣ-matrix at 1312°C where the obtained results are similar with the literature, and the cause of this difference arises from chemical composition and software database, mainly (41). Some carbide transformations such as $Cr_{23}C_6$, Cr_7C_3, and Mo_3B_2 boride formation were also expected to form during the solidification. Trace amounts of Mo_3B_2 that formed after the material is fully solidified are expected to positively affect the creep/tension rupture strength due to controlling grain coarsening during heat treatment and slowing down the grain boundary sliding mechanism.

Differently from the equilibrium cooling conditions, non-equilibrium solidification is expected to complete at 1142°C which is about 170°C lower than the equilibrium cooling as given in Table 3-b. Due to the liquid enrichment, solidification does not end when the solid composition is equal to the initial composition. Also, the solidification does not complete homogeneously since the segregation of some elements occurs during a high solidification rate.

The Scheil-Gulliver approach by assuming an infinitely high cooling rate for the given specimen has shown that

the ɣ-matrix is the former phase, which is expected to form, followed by the TiC carbides. ɣ' particles are seen beginning at 1180°C and the phase transformations are followed by Eta phase which is a metastable intermetallic that is lost as the solidification is completed. TiB2 borides are also expected to form as close to the end of solidification.

Tab.3 - Solidification modeling results completed with PANDAT™.

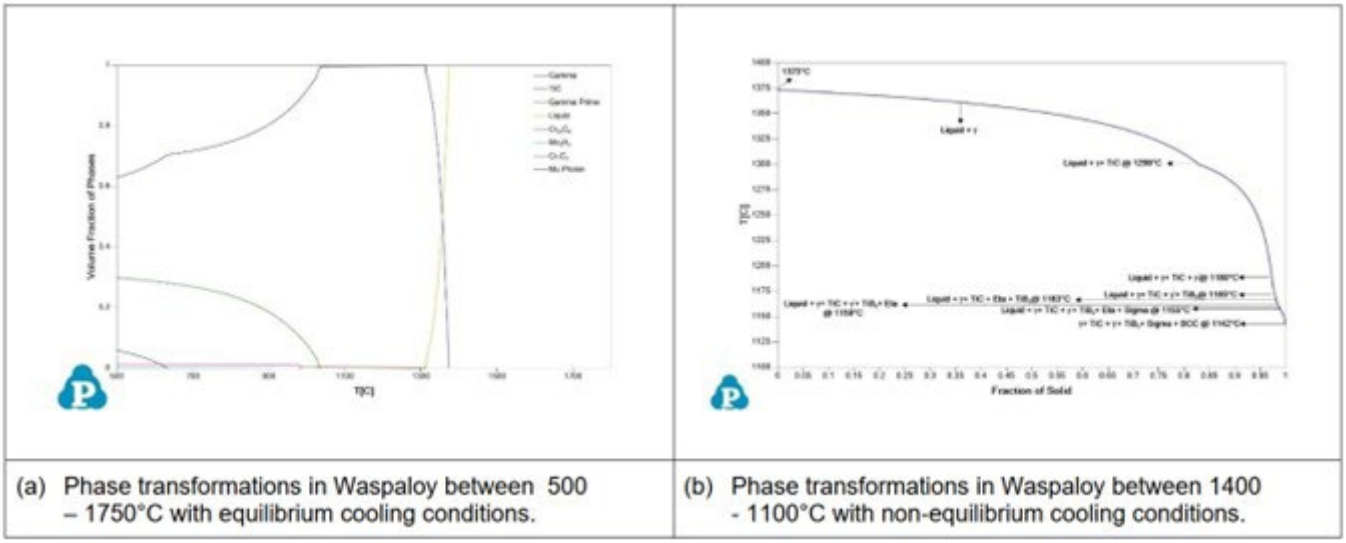

(a) Phase transformations in Waspaloy between 500 – 1750°C with equilibrium cooling conditions.

(b) Phase transformations in Waspaloy between 1400 - 1100°C with non-equilibrium cooling conditions.

SEM analysis completed on 5 specimens and on 5 different locations in each specimen has shown that the material had undergone heat treatment since ɣ' precipitates are seen in the microstructure as can be observed in Figure 1. On the other hand, SEM and EDS analysis has shown that the as-received material contains TiC and MoC carbides through the material on grain boundaries varying between 0.05 to 1.5 μm size with almost spherical morphology. ɣ' precipitates were seen in two different morphologies: cuboidal and spherical.

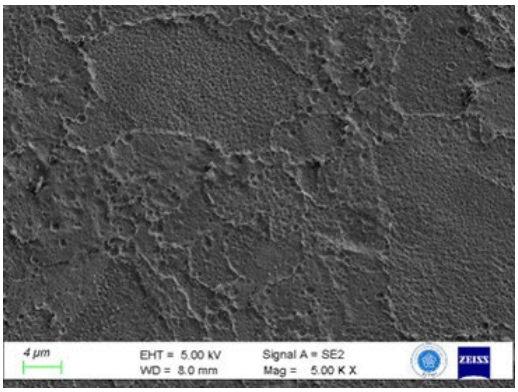

Fig. 1 - Matrix SEM image with SE detector taken under 5000X magnification with ɣ and ɣ'.

Spherical phase particles' diameter varies between 20 to 90 nm, whereas cuboidal ɣ' precipitates are found in the microstructure between 30 to 200 nm. Hardness measurements from those five specimens with 5 points in each have a result of 454.6 ±6.5 HV, which corresponds to about 1360 MPa tensile strength at room temperature. This measurement has also shown that the as-received part has undergone an aging process after wrought condition compared to the commercial-aged Waspaloy specimens seen in the literature (42-44).

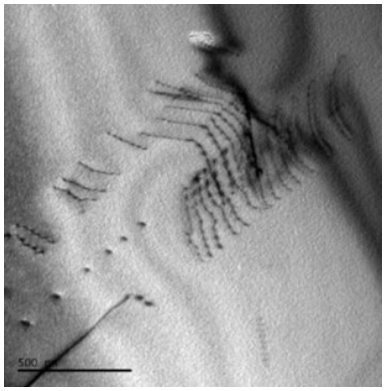

Fig. 2 - Matrix SEM image with SE detector taken under 5000X magnification with ɣ and ɣ'.

The equilibrium and non-equilibrium solidus temperatures are considered as the lower and upper end states for solidification. This approach is widely used for the estimation of solidification structures and, accordingly, for the design of the homogenization process. The solutionizing temperature is set as 1080°C and the related modeling studies have shown that the material contains only ɣ-matrix with 99.67 volume fraction and TiC particles with 0.33 volume fraction is expected at that temperature. TEM images have shown that total solutionizing of ɣ' particles occurred, dislocation pileups were observed on the grain boundary, and partial dislocations were found in the ɣ-matrix as given in Figure 2

As the modeling that is done with respect to KWN nucleation and growth has shown a volume fraction of 22 % of ɣ' particles are expected in the material (Table 4-a), TEM analysis has shown that the ɣ' precipitates are found in the microstructure with about 80.9 area percent..

Tab.4 - Isothermal aging modeling outputs (a-c) and TEM image of the specimen that aging is applied physically.

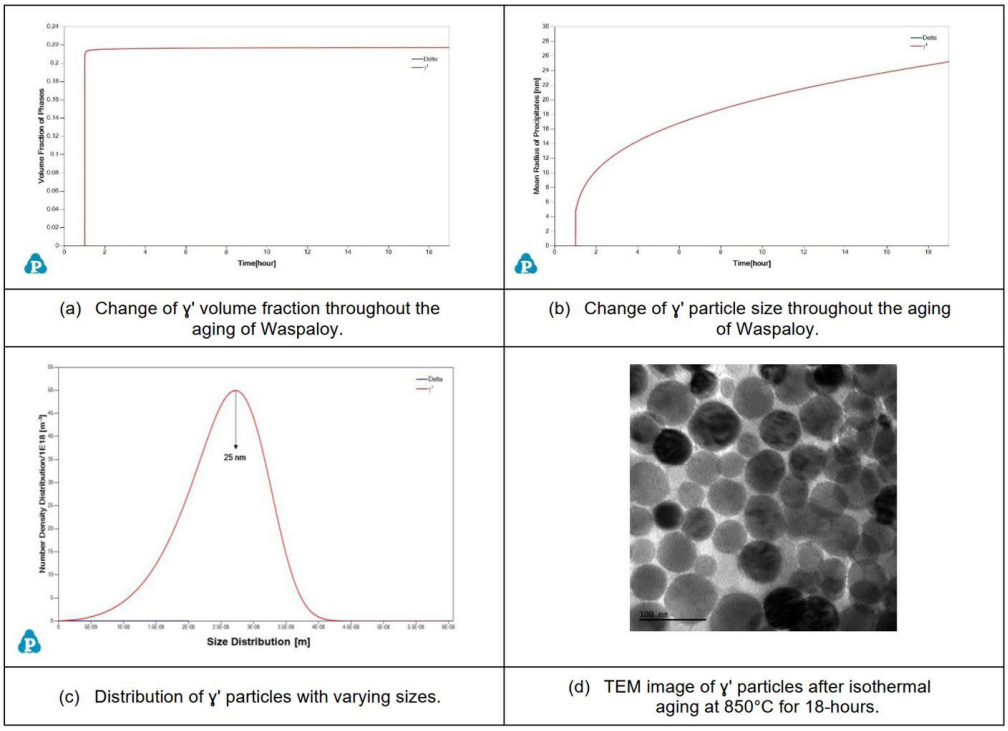

(a) Change of ɣ' volume fraction throughout the aging of Waspaloy.

(b) Change of ɣ' particle size throughout the aging of Waspaloy.

(c) Distribution of ɣ' particles with varying sizes.

(d) TEM image of ɣ' particles after isothermal aging at 850°C for 18-hours.

Although the fraction of γ' precipitates did not reflect the real heat treatment process as understood from the TEM images, the size of the γ' particles was predicted almost the same as the aging process continues. Both the simulation and TEM analysis gave similar results for γ' precipitate radius of 24.8 nm and 25.2 nm, respectively as shown in Table 4. However, although the simulation setup is prepared for homogeneous nucleation and growth, from the TEM images the nucleation characteristic is seen as semi-homogeneous in the microstructure. Lastly, although the model expected a wider LSW distribution for the radius of the particles with varying sizes, TEM analysis has shown a narrower size distribution mainly focusing on 18 to 30 nm γ' particles.

With respect to the equations described before, yield strength estimation at different temperatures is completed by using the outcomes obtained in modeling studies conducted with PANDAT™. In order to complete the yield strength predictions at elevated temperatures more accurately, some terms such as lattice strength of pure Nickel, Poisson's ratio, shear modulus, Burger's vector, lattice parameters of γ-matrix and γ' particles, interparticle spacing and k_y parameters were calculated by using JMatPro software from room temperature to elevated temperatures and used in the yield strength modeling as a function of temperature. The model parameters used for the determination of the effect of strengthening mechanisms and overall yield strength are given in Table 5, below.

Tab.5 - Model parameters for strengthening mechanisms.

Used Parameters	Numeric Value
Lattice strength of pure Ni: σ_0	69 MPa @ RT
Poisson's Ratio: v	0.26 @ RT
Shear Modulus: G	80 GPa @ RT
Burger's vector	2.04 Å at RT (a/2<110>)
Interparticle spacing: λ	36.31 nm @ RT [7]
Lattice Parameter of γ	3.59 @ RT
Lattice Parameter of γ'	3.57 @ RT
γ' radius	25 nm
γ' volume fraction	22 volume %
k_y (T)	250.36 - 0.0738T
Grain size: D	35 μm

As the critical radius is stated as 10*b by Kelly et al. (45). the critical radius for this procedure is obtained as 2.5 nm whereas the γ' particles after 18 hours aging at 850°C are expected to have a 25 nm mean radius. Thus, dislocations moving along the matrix favor Orowan looping since the particle radius is greater than the critical radius.

Additionally, although the γ' particles are expected to show coherent and homogeneous nucleation on the γ- matrix, the growth of these precipitates changes the interface characteristic from coherent to semi-coherent and incoherent (46). Therefore, coherency strengthening is also calculated and found as much effective as precipitation hardening mechanism to the yield strength of Waspaloy with the applied heat treatment.

Solid solution strengthening calculations are completed by using the solidification model results under equilibrium cooling with the elements Cr, Co, Mo, Fe, and Al to the Nickel matrix and by using the solid solution hardening coefficients found in the literature (26).

The least effective mechanism among the others is found to be grain-size hardening. In the literature, it is observed

that the grain size of Waspaloy changes from 30 to 90μm (47-49). Variation of the grain size affects the hardening due to the increasing/decreasing length of grain boundaries interacting with dislocations. However, the grain size range of Waspaloy indicated above is calculated to cause a very little difference in strength as between 24 to 42 MPa where the as-received ingot with an average grain size of 35 μm is expected to have 38.6 MPa strength from grain size hardening.

Lastly, the lattice strength of nickel is calculated as a function of temperature. Due to the Shockley partials in the material, the lattice strength of nickel decreases as the temperature increases.

By considering the fraction of these precipitates in the microstructure, it can be said that the matrix strength arises from the solid solution strengthening, grain size hardening, and matrix lattice strength whereas the second phase provides strength due to the formation of dislocation looping. Lastly, the alloy strength also increases from the interaction between the matrix and precipitates as in coherency strengthening. The contributions of all strengthening mechanisms calculated by using the outputs of modeling studies are given in Figure 3.

For the experiments applied with 0.001 strain rate, it has been seen that the room temperature properties of the material are superior to the ones at elevated temperatures in terms of both in yield and ultimate tensile strength.

After that, the property of this alloy shows better deformation kinetics and strength at 650°C than 580°C and 720°C. This also explains the design criteria of this alloy where it operates in the turbines generally around 650°C. The modeling and experimental results have shown a good agreement varying from 7 to 55 MPa from room temperature to operating temperatures.

These differences are expected to occur due to the carbides and borides formed during solidification and the heterogeneities in the microstructure where in the model the microstructure is assumed to be homogeneous.

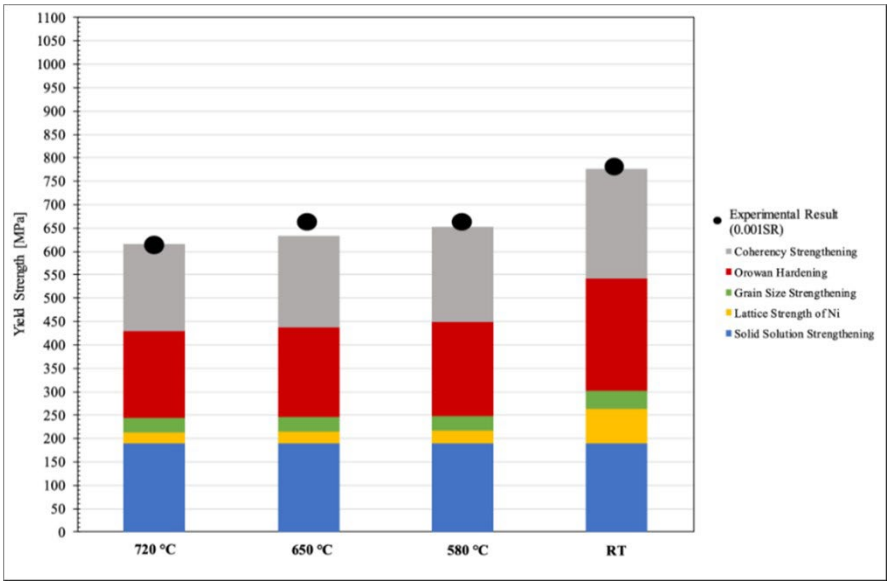

Fig. 3 - Yield strength results from modeling studies and experiments.

CONCLUSION

The effect of heat treatment on yield strength for polycrystalline Waspaloy was investigated and the corresponding modeling studies have shown that heat treatment applications with the parameters set by considering the related thermodynamic modeling results constitute around 60 % of the overall yield strength. The yield strength of Waspaloy from room temperature to operational conditions also shows that the matrix strength is mainly composed of solid solution hardening, grain boundary strengthening, and lattice strength of nickel. Linear summation of the contributions of each of these strengthening mechanisms gave a correlation with less than 8% variation with the experimental data where the

microstructural modeling results have also shown a good agreement with experimental analysis results. The given model can be used for the determination of compositional and microstructural changes 'effect on yield strength. However, more polycrystalline alloys with ɣ' precipitates should be investigated to create a generic approach that can be applied to a larger group of Ni-based superalloys.

ACKNOWLEDGEMENT

We thank CompuTherm-PANDAT™ for providing the related licences for this study. We also thank Lukasiewicz Research Network – Institute for Ferrous Metallurgy for supporting the thermomechanical tests conducted with Gleeble system and Fatih Kalıp Makine San. for the specimen preparation for Gleeble tests.

REFERENCES

[1] R. Noroozian and P. Asgharian, "Microturbine Generation Power Systems", Distributed Generation Systems: Design, Operation and Grid Integration, Elsevier, pp. 149–219, 2017.
[2] D. Raynor, J.M. Silcock, Strengthening mechanisms in γ′ precipitating alloys, Metal Sci. J. 4 (1) 1970) 121–130.
[3] V. Gerold, H. Haberkorn, On the critical resolved shear stress of solid solutions containing coherent precipitates, Phys. Status Solidi B 16 (2) (Jan 1966) 675–684.
[4] R.F. Decker, J.R. Mihalisin, Coherency strains in γ′ hardened nickel alloys, Trans. Am. Soc. Met. 62 (1969) 481–489.
[5] R.F. Miller, G.S. Ansell, Low temperature mechanical behavior of Ni-15Cr-Al-Ti-Mo alloys, Metall. Trans. A. 8 (12) (1977) 1979–1991.
[6] E.J. Lee, A.J. Ardell, Superposition of precipitation-hardening mechanisms, in: P. Haasen, V. Gerold,
[7] G. Kostorz (Eds.), Strength ofMetals and Alloys, vol. 1, PergamomPress 1979, pp. 633–638.
[8] A. Melander, P.A. Persson, Strength ofγ′ hardened nickel-base alloy, Met. Sci. 12 (9) (1978) 391–398.
[9] V.A. Phillips, Hardening mechanisms in a precipitation hardenable nickel-12.71 at.% aluminium alloy, Philos. Mag. 16 (139) (1967) 103–117.
[10] L.K. Singhal, J.W. Martin, The mechanism of tensile yield in an age-hardened steel containing γ′ (ordered Ni3Ti) precipitates, Acta Metall. 16 (7) (1968) 947–953.
[11] E.I. Galindo-Nava, L.D. Connor, C.M.F. Rae, On the prediction of the yield stress of unimodal and multimodal γ′ nickel-base superalloys, Acta Mater. 98 (2015) 377–390.
[12] R.W. Kozar, A. Suzuki, W.W. Milligan, J.J. Schirra, M.F. Savage, T.M. Pollock, Strengthening mechanisms in polycrystalline multimodal nickel-base superalloys, Metall. Mater. Trans. A 40 (2009) 1588–1603.
[13] "Standard Practice for Microetching Metals and Alloys", ASTM International, 1999.
[14] U. R. Kattner, "The Calphad Method and Its Role in Material and Process Development", Tecnologia em Metalurgia Materiais e Mineracão, vol. 13, no. 1, pp. 3–15, 2016.
[15] Rahimian, M., Milenkovic, S. & Sabirov, I. Microstructure and hardness evolution in MARM247 Ni-based superalloy processed by controlled cooling and double heat treatment. J. Alloys Compd. 550, 339–344 (2013).
[16] Hammadi, S. Solidification Modeling of Microsegregation. 30 (2018).
[17] Wolff, I. M. Precipitation accompanying overheating in nickel-base superalloy. Mater. Charact. 29, 55– 61 (1992).
[18] Z. Sheng, M. Bonvalet Rolland, T. Zhou, J. Odqvist, and P. Hedström, "Langer–Schwartz–Kampmann– Wagner precipitation simulations: assessment of models and materials design application for Cu precipitation in PH stainless steels", Journal of Materials Science, vol. 56, no. 3, pp. 2650–2671, Jan. 2021.
[19] C. Sommitsch, E. Kozeschnik, G. Wasle, and B. Buchmayr, "A Precipitation Model for Multi-Component Multi-Phase Systems in Nickel-Base Superalloys", 2000.
[20] Y. H. Wen, B. Wang, J. P. Simmons, and Y. Wang, "A phase-field model for heat treatment applications in Ni-based alloys", Acta Materiala, vol. 54, no. 8, pp. 2087–2099, May 2006.
[21] K. Zhang, F. Yu, M. Zhu, J. Dan, X. Wang, J. Zhang, B. Dai, "Enhanced low temperature NO reduction
[22] performance via MnOx-Fe2O3/vermiculite monolithic honeycomb catalysts", Catalysts, vol. 8, no. 3, Mar. 2018.
[23] M. Bonvalet, T. Philippe, X. Sauvage, and D. Blavette, "Modeling of precipitation kinetics in multicomponent systems: Application to model superalloys", Acta Materiala, vol. 100, pp. 169–177, Nov. 2015.
[24] R. Wagner, R. Kampmann, and P. W. Voorhees, "Homogeneous Second-Phase Precipitation", 1986
[25] A. J. Ardell, "Precipitation Hardening", 1985.
[26] L. Brown and R. Ham, "Dislocaton-particle interactions in Kelly, A and Nicholson, RB.", Strengthening methods in crystals, J. Wiley and Sons, 1971.
[27] A. Kelly and K. B. Nicholson, "Precipitation hardening", Progress in Materials Science, vol. 10, Macmillan, 1963.
[28] A. J. Goodfellow, E. I. Galindo-Nava, C. Schwalbe, and H. J. Stone, "The role of composition on the extent of individual strengthening mechanisms in polycrystalline Ni-based superalloys", Materials and Design, vol. 173, Jul. 2019.

[29] R. W. Kozar, A. Suzuki, W. W. Milligan, J. J. Schirra, M. F. Savage, and T. M. Pollock, "Strengthening mechanisms in polycrystalline multimodal nickel-base superalloys", Metallurgical and Materials Transactions A: Physical Metallurgy and Materials Science, vol. 40, no. 7, pp. 1588–1603, 2009.
[30] T. Zhou, P. Hedstr m, D. San Martin, "Integrated Experimental and Computational Study of Precipitation in Martensitic Steels", KTH Royal Institute of Technology, 2019.
[31] H. Wen, T. D. Topping, D. Isheim, D. N. Seidman, and E. J. Lavernia, "Strengthening mechanisms in a high-strength bulk nanostructured Cu-Zn-Al alloy processed via cryomilling and spark plasma sintering", Acta Materiala, vol. 61, no. 8, pp. 2769–2782, May 2013.
[32] V. Gehold and H. Habehkorn, "On the Critical Resolved Shear Stress by of Solid Solutions Containing Coherent Precipitates", 1966.
[33] R. L. Fleischert, "Substitutional Solution Hardening", 1963.
[34] A. Argon, Strengthening Mechanisms in Crystal Plasticity, Oxford University Press, 2007.
[35] R. W. Cahn and P. Haasen, Physical Metallurgy, 4th edition. North Holland, 1996.
[36] G. E. Dieter, Mechanical Metallurgy, 1988.
[37] M. Al-saadi, F. Sandberg, P. G. Jönsson, and C. N. Hulme-smith, "Modelling of strengthening mechanisms in wrought nickel-based 825 alloy subjected to solution annealing", Metals (Basel), vol. 11, no. 5, 2021.
[38] Y. Mishima, S. Ochiai, N. Hamao, M. Yodogawa, and T. Suzuki, "Solid Solution Hardening of Nickel-Role of Transition Metal and B-subgroup Solutes", 1986.
[39] E. I. Galindo-Nava, L. D. Connor, and C. M. F. Rae, "On the prediction of the yield stress of unimodal and multimodal γ′ Nickel-base superalloys", Acta Materiala, vol. 98, pp. 377–390, Aug. 2015.
[40] R. Labusch, "A Statistical Theory of Solid Solution Hardening a Statistical Theory of Solid Solution Hardening", 1970.
[41] W. D. Callister and D. G. Retwisch, Materials Science and Engineering: An Introduction, 10th edition, Wiley, 2018.
[42] S. Utada, R. Sasaki, R. C. Reed, and Y. T. Tang, "Overheating of Waspaloy: Effect of cooling rate on flow stress behavior", Materials and Design, vol. 221, Sep. 2022.
[43] 41.W.-D. Cao, "US6730264", US 6,730,264 B2, May 04, 2004.
[44] 42.M. A. Neri, A. Martinez -Villafañe, C. Carreño, A. D. Gonzalez Escarcega, O. Cobarrubias-Alvarado, "Metallurgical Characterization of Waspaloy Presenting Variations in Chemical Composition, Grain Size and Hardness", The Minerals, Metals & Materials Society, 2012.
[45] 43.I. Dempster, W.-D. Cao, R. Kennedy, B. Bond, J. Aurrecoechea, and M. Lipschutz, "Structure and Property Comparison of Allvac ® 718plus Alloy and Waspaloy Forgings", The Minerals, Metals & Materials Society, 2005.
[46] 44.A. Chamanfar, "Evolution of Microstructure and Mechanical Properties in Linear Friction Welded Waspaloy", 2012.
[47] 45.A. Kelly and R. B. Nicholson, Strengthening methods in crystals, no. 4. Elsevier BV, 1971.
[48] 46.R. W. Hertzberg, Deformation and Fracture Mechanics of Engineering Materials, 4th edition. Wiley and Sons Inc, 1996.
[49] 47.R. F. Decker, A. I. Rush, A. G. Dano, J. W. Freeman, "Abnormal Grain Growth in Nickel-Base Heat Resistant Alloys", 1956.
[50] 48.J. Moravec, "Determination of the grain growth kinetics as a base parameter for numerical simulation demand", MM Science Journal, vol. 2015, pp. 649–653, Oct. 2015.
[51] 49.M. A. Neri, A. Martinez -Villafañe, C. Carreño, A. D. Gonzalez Escarcega, O. Cobarrubias-Alvarado, "Metallurgical Characterization of Waspaloy Presenting Variations in Chemical Composition, Grain Size and Hardness", The Minerals, Metals & Materials Society, 2012.

TORNA ALL'INDICE >